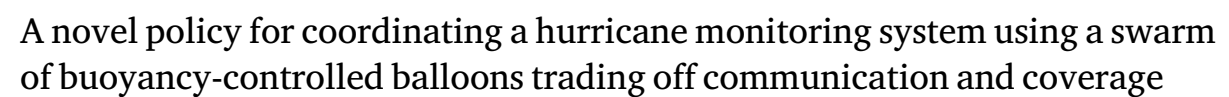
ELSEVIER

Contents lists available at ScienceDirect

Engineering Applications of Artificial Intelligence

journal homepage: www.elsevier.com/locate/engappai







Bruno R.O. Floriano ^{a,*}, Benjamin Hanson ^b, Thomas Bewley ^b, João Y. Ishihara ^a, Henrique C. Ferreira ^a

- a Universidade de Brasília (UnB), Departamento de Engenharia Elétrica, Campus Universitário Darcy Ribeiro, 70910-900 Brasília-DF, Brazil
- b Mechanical and Aerospace Engineering, University of California San Diego, 1805 EBU1 (Jacobs Hall), San Diego, 92093-0411, CA, United States

ARTICLE INFO

Keywords: Hurricane monitoring Multi-agent system Weather forecast Buoyancy-driven balloons Neural network based model predictive control

ABSTRACT

This paper introduces a novel architecture for hurricane monitoring aimed at maximizing the collection of critical data to enhance the accuracy of weather predictions. The proposed system deploys a swarm of controllable balloons equipped with meteorological sensors within the hurricane environment. A key challenge in this setup is managing the trade-off between maximizing area coverage for data collection and maintaining robust communication links among the balloons. To address this challenge, we propose a cost function with two conflicting components: one prioritizes area coverage, and the other focuses on repositioning to maintain communication. This cost function is optimized using an adaptive neural network-based model predictive control strategy, which enables the system to dynamically balance these competing requirements in real-time. Quantitative results from extensive simulations demonstrate the versatility and effectiveness of the proposed architecture, showing that it can achieve comprehensive communication connectivity and increased area coverage across various configurations, including different numbers of balloons and operational periods.

1. Introduction

On-site monitoring of extreme natural phenomena, particularly hurricanes, plays a crucial role in acquiring essential data for accurate forecasting (Meneghello et al., 2016). Correctly anticipating such weather conditions can enable preventive responses that effectively safeguard lives (Bewley and Meneghello, 2016). Efficient on-site monitoring can be achieved by deploying multiple Unmanned Aerial Vehicles (UAVs) at the site of the occurrence (Cione et al., 2016; Stampa et al., 2021; Mohsan et al., 2023). Utilizing Multi-Agent Systems (MAS) enhances the volume of accessible information, including speed profiles, temperature, pressure, and other sensor data, due to their expanded coverage capacity (Floriano et al., 2021). For instance, numerous studies in recent years have explored the use of UAV swarms for monitoring wildfires or floods (Lin and Liu, 2018; Hu et al., 2022; Tzoumas et al., 2023; Viseras et al., 2021; Afghah et al., 2019; Seraj et al., 2022; Baldazo et al., 2019).

When it comes to monitoring hurricane-affected areas, recent studies have presented UAV solutions utilizing quadrotors. For example, the impacts of Hurricanes Harvey and Irma in the United States in 2017 were accompanied by numerous studies investigating their effects on roads, buildings, and cities (Greenwood et al., 2020; Yeom et al.,

2019; Rojas et al., 2022; Congress et al., 2019). Similar investigations were conducted for other recent incidents, such as Hurricane Willa (Vizcaya-Martínez et al., 2022) and Hurricane Maria (Schaefer et al., 2020), employing these types of vehicles. However, as outlined in the survey conducted by Mohsan et al. (2023), operating quadrotors in adverse weather conditions like hurricanes remains a significant challenge due to operational complexities and difficulties in obtaining precise data. Furthermore, both quadrotors and fixed-wing aircraft often face limitations in terms of flight duration due to their energy requirements (Meneghello et al., 2016).

Our team has proposed to monitor hurricanes by employing low-cost buoyancy-driven balloons equipped with sensors, enabling prolonged monitoring operations for several days (Meneghello et al., 2017). Bewley and Meneghello (2016) proposed an innovative monitoring system with a swarm of balloons assuming a pre-defined fixed orbit for each balloon. Meneghello et al. (2018) proposed a simple three-level control (TLC) rule which enables to place a single balloon in any desired position in a hurricane area. However, an integrated system with an efficient automatic positioning of several balloons is still missing.

One important aspect in designing a cooperative UAV system is the communication between the UAVs. Note that the difference between a

E-mail address: bruno.floriano@aluno.unb.br (B.R.O. Floriano).

^{*} Corresponding author.

hurricane's area (around a 200 km radius) (Holland et al., 2010) and the range of long-range (LoRa) communication technology (up to 10 km) (Sanchez-Iborra and Cano, 2016) is significant. This difference could jeopardize the UAV ability to maintain constant connectivity. Several studies have explored multi-agent monitoring systems with intermittent communication (Hu et al., 2018; Shi et al., 2023; Wen et al., 2014; Xiao and Dong, 2021; Zhang et al., 2021). However, to the best of the authors' knowledge, none have established a control architecture to address the trade-off between area coverage and communication.

On the subject of intelligent updating processes, recent research in artificial intelligence (AI) has significantly contributed to modeling natural phenomena (Sabir et al., 2024b,c). For instance, the work of Sabir et al. (2024b,c) presents a neural network-based model to analyze the dynamics of Zika virus transmission and its interactions with humans, non-human primates, and mosquito vectors. Similarly, AI approaches have also contributed to medical applications, such as surgeries (Sabir et al., 2024d). The work of Sabir et al. (2024d) introduces a novel approach to modeling corneal shape-based eye surgery, which is crucial for understanding and addressing various visual impairments. Finally, the capacity of neural networks is also demonstrated in works such as Sabir et al. (2024a), which designed stochastic solvers for solving the fifth-order Emden-Fowler system (FOEFS) of equations. This type of solution has several applications in engineering and science.

This is also true in the context of multiple UAVs, where similar techniques have been employed to tackle challenges related to coverage, monitoring, and communication (Manoharan and Sujit, 2022; Eshaghi et al., 2023; Day and Salmon, 2021; Puente-Castro et al., 2022; Fuertes et al., 2023; Wu et al., 2023). These studies have explored various aspects of UAV operations, including cooperative target defense and coverage (Manoharan and Sujit, 2022), concurrent planning with different objectives (Eshaghi et al., 2023), position allocation (Wu et al., 2023), and path planning (Puente-Castro et al., 2022; Fuertes et al., 2023). Additionally, swarm intelligence algorithms have been recognized for their role in facilitating collaboration among multiple UAVs (Tang et al., 2023). AI-based approaches, such as multiobjective evolutionary optimization (Ramirez-Atencia and Camacho, 2019), have shown promise in addressing conflicting objectives and enhancing mission planning. Furthermore, AI algorithms have been applied to MAS problems, effectively managing UAV trajectories, optimizing load distribution, and enabling targeted communication (Queralta et al., 2020; Wang et al., 2020; Das et al., 2019). However, none of these solutions have simultaneously addressed the issues of intermittent communication while maximizing area coverage.

In terms of AI approaches for MAS applications, Neural Network Model Predictive Control (NNMPC) has been introduced as an online, multi-agent, single-objective solution (Floriano et al., 2022) The motivation behind using the proposed NNMPC method stems from its adaptive capabilities and predictive strengths, which are well-suited to address the dynamic and evolving nature of the problem. The NNMPC framework is particularly advantageous because it allows the system to continuously adjust to the ever-changing conditions as they occur within the hurricane environment. The adaptive characteristics of the neural network enable the control system to respond in real time to fluctuations in both communication needs and area coverage demands. Moreover, the predictive capacity of the Model Predictive Control (MPC) component plays a key role in anticipating potential changes and making informed decisions about the system's future states. By forecasting the evolution of the hurricane and the corresponding shifts in areas of interest, the NNMPC can proactively manage the trade-offs between coverage and communication. This forward-looking approach ensures that the system is not merely reactive but is strategically positioned to gather the most critical data while maintaining effective communication links.

In our approach, we adapt Neural Network Model Predictive Control (NNMPC) to manage the competing objectives of hurricane monitoring. This real-time control system dynamically adjusts to continuously

changing conditions, ensuring the best possible control decisions. To handle the trade-off between communication and area coverage, we propose a control architecture that utilizes a cost function that effectively balances these elements. Specifically, the area of interest is updated over time using the Fokker–Planck equation, which tracks the freshness of data from different regions. Meanwhile, communication needs are addressed with a linear decay model to efficiently allocate resources. This setup allows the system to respond flexibly and optimally to evolving monitoring challenges.

To summarize, this paper contributes in the following:

- It expands the application of buoyancy-driven balloons in a stratified flowfield, as explored by Meneghello et al. (2016, 2018) (which was restricted to a single balloon), to multiple agents, thereby increasing area coverage and data collection.
- It extends the swarm architecture of Bewley and Meneghello (2016) with fixed desired orbits by implementing a communication routing mechanism and establishing an intelligent control strategy that chooses the best orbits for optimizing area coverage and data flow.
- It builds, specifically for hurricane-relevant data monitoring, a weighted cost function for conflicting objectives to effectively balance area coverage with repositioning for connectivity.
- Establishes a constant restoring interest function, driven by the Fokker–Planck equation, to characterize the need for updating previously covered regions after a certain period.

Quantitative results from extensive simulations underscore the effectiveness of the proposed architecture, demonstrating comprehensive communication connectivity and the ability to cover a significant proportion of the targeted area across different operational windows and varying numbers of balloons. These outcomes not only validate the robustness of our approach but also highlight the system's efficiency in achieving the dual objectives of comprehensive data acquisition and reliable information transmission. In the demanding and dynamic environment of hurricane monitoring, where timely and accurate data are critical, the demonstrated capabilities of our system represent a significant advancement, offering a promising solution to the complex challenges inherent in this field.

This paper is organized as follows: Section 2 describes the system dynamics and the problem's objectives; Section 3 details the control architecture based on NNMPC optimization; Section 4 presents the simulation results and evaluates the overall performance of the system; and Section 5 provides concluding remarks.

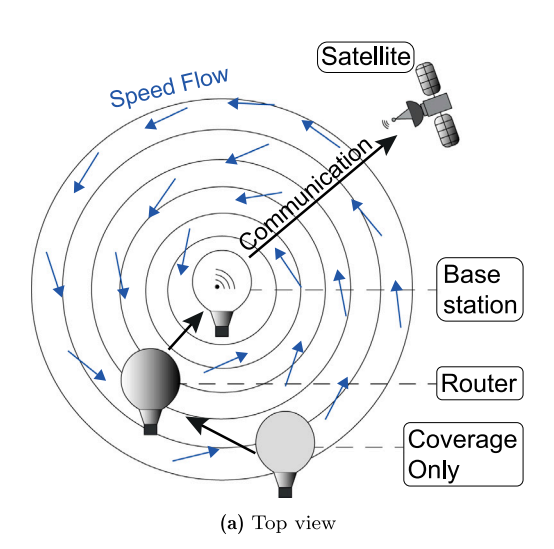
2. Preliminaries and problem formulation

2.1. Monitoring system general configuration

We assume a hurricane monitoring system consisting of a swarm of functionally heterogeneous UAVs navigating within a hurricane flow field, as illustrated in Fig. 1.

The objective of the system is to cover a significant portion of the hurricane-affected areas (to be defined later), collect sensor data such as wind speed, pressure, and temperature, and transmit this data to a satellite.

Considering that the maximum communication range between a sender and a receiver is much smaller than the dimensions of the hurricane area to be covered, multiple UAVs are deployed with functionalities distributed among base stations, routers, or coverage-only units. Due to the limited hardware capacity of small UAVs, equipping all of them with the necessary gear for satellite communication is impractical. Therefore, our communication goal is for all UAVs to transmit their data to a central agent, referred to as the base station or simply the base. The base station is a robust agent with enhanced hardware that collects information from all UAVs and connects directly to a satellite to transmit the collected data.



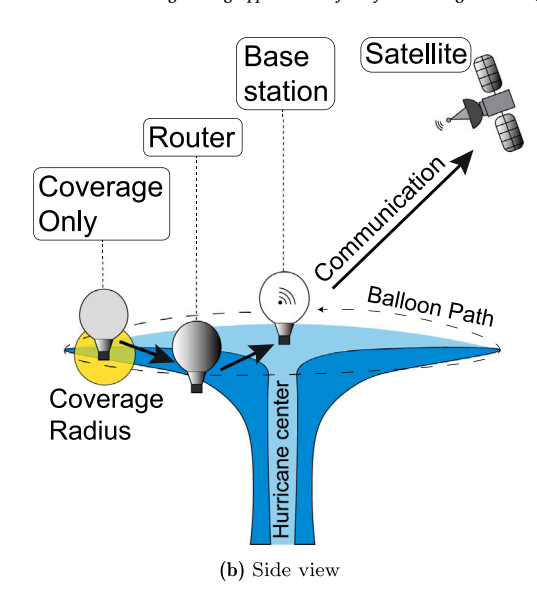


Fig. 1. Description of the balloon swarm in a hurricane.

The geometrical distribution of the UAVs considers area coverage, energy consumption, and communication capability. To enhance fuel economy and long-term autonomy, we assume that balloons are used as UAV units. Once a balloon is positioned within the hurricane, it is naturally carried by the hurricane's flow field, resulting in circular trajectories and no fuel consumption, as illustrated in Fig. 1. In its ideal geometric configuration, we assume the swarm has the base station at the center of the hurricane. Surrounding the hurricane's periphery are coverage agents, focused solely on collecting sensor data within their designated areas. Bridging these coverage agents and enabling efficient data transmission are the routers—balloons equipped with both coverage and routing capabilities. These routers facilitate the transfer of information from the other balloons to the base station.

Any initially given swarm geometric configuration changes naturally, as each balloon is carried along the hurricane's flow trajectory at different velocities. Consequently, the roles of the balloons as routers or coverage units must adapt over time based on their positions. This role adjustment is managed by a routing protocol detailed in Section 2.2.1.

To ensure timely coverage of the hurricane area, two potential solutions are possible: deploying a significantly large number of UAVs to maintain easy neighbor connectivity or designing a control strategy that periodically brings the UAVs closer together to facilitate data routing to the base station. The latter approach was chosen because it requires fewer UAVs, thereby reducing costs. The radial distance of each balloon from the base is automatically adjusted by a control subsystem embedded in the monitoring system, as described in Section 3.

In summary, the proposed structure enables a relatively small number of cost-effective vehicles to efficiently share valuable information with the satellite while maximizing area coverage and minimizing fuel consumption.

2.2. Communication

The communication technology selected for the proposed hurricane monitoring system is LoRa (Long Range), chosen for its low power consumption, extensive range capability (Sanchez-Iborra and Cano, 2016), and proven effectiveness in UAV-based disaster monitoring applications (Saraereh et al., 2020). LoRa's low power consumption is crucial for ensuring that the balloons remain cost-effective and can operate for extended durations, thereby enabling broader coverage of the hurricane area. Its extensive range, which can reach up to 10

km (Petajajarvi et al., 2015), is essential for covering the vast scale of a hurricane, which can extend up to 200 km (Holland et al., 2010).

In the next subsection, we present our proposed routing protocol. By accommodating changing communication graphs, the protocol leverages established LoRa network practices from the literature (Ghazali et al., 2021).

2.2.1. Routing protocol

A routing protocol is an algorithm that determines the configuration of communication paths among the system's agents. The choice of protocol impacts the extent of long-range communication, the total area covered, and power consumption. Inspired by the tree-based routing protocol, which was designed as a power-aware protocol by Gong and Jiang (2011), we propose a minimum-cost routing protocol, as detailed in Algorithm 1.

In Algorithm 1, we assume that the communication range $\rho > 0$ between any two balloons is known. Balloon 1 is designated as the base station (base), and the remaining balloons $2, \ldots, N$ are positioned along several concentric circles around the base, as shown in Fig. 1. A balloon j can only send data to an agent i that is closer to the base station than itself. The protocol aims to establish a communication link for each non-base balloon j, either directly to the base or to another balloon i that is closer to the base and can function as a router to the base.

As input information, the algorithm uses the horizontal distance between each pair of balloons

$$d_{ij}(t) = \|q_i(t) - q_j(t)\|,\tag{1}$$

where $q_i(t)$ represents the horizontal position of the ith balloon, as detailed in (5). Note that a communication connection from j to i is possible only when they are within the communication range, that is, at time instants t such that $d_{ij}(t) < \rho$. The algorithm prioritizes establishing communication with the base for all balloons j within the base station's communication range ρ . For each balloon j that cannot connect directly to the base station, the algorithm seeks a possible router among balloons i that are closer to the base (i.e., $d_{1i} < d_{1j}$) and within the connectivity range, meaning $d_{ij} < \rho$. To reduce the number of communication nodes and energy consumption, the algorithm selects as a router the balloon i with the lowest cost C_{ij} . The cost function C_{ij} can be a general function relating to communication

 $^{^{1}\,}$ We assume the range for the vertical position z is small compared to the horizontal distances.

Algorithm 1 Routing protocol

```
1: Input: d_{ij} [distance between the balloons i, j \in \{1, ..., N\}]
 2: Parameter: \rho > 0 [communication range]
 3: Initialization: l_{ij} = 0, \forall i, j \in \{1, ..., N\}
 4: for j = 2, ..., N do
         if d_{1i} < \rho then
 5:
 6:
            l_{1i} \leftarrow -1 [balloon j within the base range is connected to
     the base]
 7:
         else
 8:
             C_{min,j} = d_{1j}
             p = 0 [p is the balloon outside base range that is closest to
 9:
     j
              for i = 2, ..., N, i \neq j do
10:
                  if d_{ij} < \rho then
11:
                      C_{ij} \leftarrow d_{ij}

if (d_{1i} < d_{1j}) & (C_{ij} < C_{min,j}) then
12:
13:
                           C_{min,j} \leftarrow C_{ij}

p \leftarrow i \ [p \text{ must be closer to the base than } j]
14:
15:
                       end if
16:
                  end if
17:
18:
              end for
              if p \neq 0 then
19:
                  l_{pj} \leftarrow -1 [j is connected to p]
20:
21:
22:
          end if
23: end for
24: for i = 1, ..., N do
         l_{ii} \leftarrow -\sum_{j=1}^{N} l_{ij}
25:
26: end for
27: Return: L = (l_{i,i})
```

parameters between balloons j and i, such as distance or energy. For simplicity, Algorithm 1 uses the cost $C_{ij}=d_{ij}$, as this is sufficient for demonstrating that data will be sent to the nearest balloon. An effective communication link from j to i is indicated by $l_{ij}=-1$. Algorithm 1 returns a communication architecture represented by the Laplacian matrix of the communication network, $L=(l_{ij})$. By construction, the communication graph is directed, meaning that the existence of communication from j to i does not imply that communication from i to j also exists.

2.2.2. Data storage for message forwarding

When a balloon establishes a connection with a neighboring balloon, it gains the ability to both receive and transmit data. To achieve one of the objectives outlined in Section 3.1 – ensuring maximum data accessibility for the base station – it is necessary to differentiate the roles of each balloon. To address this, we propose the concept of routing balloons, which form a distinct group of agents capable of receiving and storing data from other balloons. These routing balloons can then efficiently forward the accumulated data to the base station. This approach ensures that information reliably reaches its intended destination without compromising coverage.

Since we are using predictive control (explained in detail in Section 3.4), the system can plan ahead and determine which balloon will act as the router. This means the selected agent will handle the transmission of data either from one neighbor to another or directly to the base station

Therefore, a mathematical variable is needed to characterize the cumulative behavior of the data transmitted and stored between balloons.

Let $\bar{L}(q(t),t) \in \mathbb{R}^N$ be a cumulative Laplacian matrix. It differs from L(q(t)), which represents only the instantaneous communication graph. Instead, $\bar{L}(q(t),t)$ characterizes a cumulative graph that represents both past and present communication. In this sense, after a disconnection

between i and j, the entry \bar{l}_{ij} retains a non-zero value (indicating a past connection), while l_{ij} drops to zero immediately.

As the system is designed to operate over extended periods, a key consideration is the potential outdatedness of data stored in the routers. By the time the data reaches the base station, it may no longer be relevant or reflective of current conditions. To address this challenge and ensure periodic updating, we propose incorporating a decay factor into the cumulative Laplacian matrix. This decay factor represents the gradual degradation of stored data over time, signifying the diminishing relevance of outdated information. Consequently, the evolution of \bar{l}_{ij} can be modeled to capture the temporal dynamics and mitigate the impact of outdated data on the overall system performance, as follows

$$\bar{l}_{ij}(\boldsymbol{q}(t),t) = \begin{cases} l_{ij}(\boldsymbol{q}(t_c)), & \text{if } t_c \le t < t_d \\ l_{ij}(\boldsymbol{q}(t_c))\lambda(t-t_d), & \text{if } t \ge t_d \end{cases}$$
 (2)

where $\lambda(t)$ is a decay function, and t_c and t_d represent the connection and disconnection times, respectively. Given that the communication decay is slow enough to allow information to be stored for hours, $\lambda(t)$ can be modeled as a linear decay with a period T_{cc} , i.e.

$$\lambda(t) = \begin{cases} 1 - \frac{t}{T_{cc}}, & \text{if } 0 \le t < T_{cc} \\ 0, & \text{otherwise.} \end{cases}$$
 (3)

Finally, if at the moment of connection between i (the recipient) and j (the sender), balloon j holds information from another balloon k ($k \neq i, j$), meaning $\bar{l}_{jk} \neq 0$, then balloon j can forward this data to balloon i. In other words, $\bar{l}_{jk} = \bar{l}_{jk}$.

3. Control architecture

This section details the architecture of the proposed control system. The primary objective of this architecture is to achieve the system's goals as outlined earlier. Specifically, it is designed to manage a swarm of balloons within a hurricane zone, as described in Section 2.1, regardless of their initial geometrical distribution.

We can state the objective of the control protocol as follows:

- · Cover a significant portion of the hurricane-affected areas.
- Periodically reposition the balloons to ensure they remain within communication range of each other, thereby enabling reliable data routing.
- Route the information from the balloons until it reaches the base station.

To achieve these objectives, we propose a control system architecture as depicted in Fig. 2. The communication network is established using the routing protocol discussed in Section 2.2. In this context, the communication graph defines the path through which data flows, based on the current position of each balloon, $q_i(t)$.

As indicated in Fig. 2, based on the current positions of all balloons q(t), the NNMPC block provides each balloon with a control signal $u_i(t)$ that directs it to a new position. Following the three-level control (TLC) rule suggested by Meneghello et al. (2016, 2018), the balloon altitude must always be within one of three possible values: $\mathcal{Z} = \{-\bar{z}, 0, \bar{z}\}$. Here, 0 represents the reference altitude, and \bar{z} is the maximum altitude gap. The control signal $u_i(t)$ determines the balloon's altitude based on current needs. By adjusting its altitude, the balloon also modifies its radial position due to its dynamics, as described in Eqs. (4a) and (4b). The selection of the appropriate value for $u_i(t)$ at each time instant is managed by a neural network-based model predictive control (NNMPC) system, as introduced by Floriano et al. (2022) and detailed in Section 3.4.

For controller tuning, we first present the dynamic law of each balloon and then develop cost functions that represent the goals of coverage and communication.

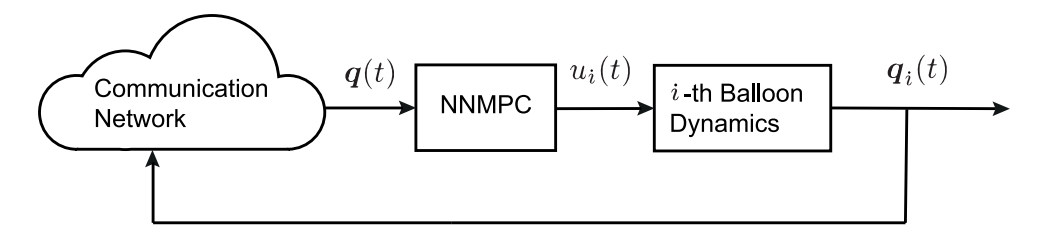


Fig. 2. Block diagram of the control architecture of the ith balloon.

3.1. Balloon dynamics

The continuous-time dynamics of the ith buoyancy-driven balloon ($i \in 1, ..., N$, where i = 1 represents the base station), adapted from Meneghello et al. (2018), are given by the following equations

$$\dot{r_i} = \alpha z_i + \xi_i,\tag{4a}$$

$$z_i = u_i, (4b)$$

$$\dot{\theta}_i = \frac{v_i}{r_i},\tag{4c}$$

$$v_i = V_m \left(\left(\frac{R_V}{r_i} \right)^{\phi} \exp \left[1 - \left(\frac{R_V}{r_i} \right)^{\phi} \right] \right)^{\chi}, \tag{4d}$$

where r_i , z_i , and θ_i denote the radial, vertical, and angular positions of the ith balloon, respectively. The variable α represents the timeaveraged vertical gradient of the radial velocity. The white Gaussian noise ξ_i accounts for fluctuations in the radial velocity due to hurricane turbulence, with zero mean and variance c^2 . The control signal is denoted by $u_i(t)$. Eq. (4c) indicates that the angular velocity is a function of the tangential velocity v_i and the radial position r_i . Eq. (4d) shows that the tangential velocity v_i depends on the balloon's position within the hurricane. In this equation, V_m represents the maximum tangential wind speed, R_V is the radius at which V_m is attained, ϕ is a shape parameter defining the proportion of pressure near the maximum wind radius, and the exponent variable χ accounts for both the maximum wind values and the data in the outer circulation. Eq. (4d) is obtained from the hurricane model, and for this work, we use the H10 model described by Holland et al. (2010), known for its low sensitivity to observing system errors.

Note from Eq. (4b) that the control variable $u_i(t)$ directly affects the vertical position of the balloon. This, in turn, influences the radial position of the balloon as described by Eq. (4a). The challenge is to determine an appropriate function $u_i(t)$ for each balloon in the swarm to achieve the objectives of the control protocol.

3.2. Relevant area coverage

The first objective of the system is to ensure relevant area coverage, meaning that the balloons should cooperatively cover the maximum area affected by the hurricane to collect the most pertinent data. To achieve this, an interest function must be defined – a function of the geographical coordinates that determines the relevance of the information to be measured at time t for every position within the hurricane.

The 2D coordinate $q_i(t) \in \mathbb{R}^2$ of the *i*th balloon at time *t* is given by

$$q_i(t) = \begin{bmatrix} r_i(t)\cos(\theta_i(t)) \\ r_i(t)\sin(\theta_i(t)) \end{bmatrix}. \tag{5}$$

The vector of all balloons' positions is defined as

$$q(t) = \begin{bmatrix} q_1(t) & \dots & q_N(t) \end{bmatrix}^T.$$
 (6)

Let $\Gamma(q(t),*,t): \mathbb{R}^2 \to \mathbb{R}$ be the interest function of the hurricane at time t, given the balloons' positions q(t). The initial distribution along $\mathbf{x} = \begin{bmatrix} x_1 & x_2 \end{bmatrix}^T \in \mathbb{R}^2$ for the interest function is given by

$$\Gamma(\boldsymbol{q}(0), \boldsymbol{x}, 0) = \frac{1}{(2\pi |\boldsymbol{\Sigma}|)^{1/2}} \exp\left[-\frac{1}{2} \left(\left(\boldsymbol{x} - \boldsymbol{\mu} \right)^T \boldsymbol{\Sigma}^{-1} \left(\boldsymbol{x} - \boldsymbol{\mu} \right) \right)^2 \right], \tag{7}$$

where $\mu = \begin{bmatrix} 0 & 0 \end{bmatrix}^T$ is the position of the hurricane's center, and $\Sigma = \sigma^2 \begin{bmatrix} 1 & 0 \\ 0 & 1 \end{bmatrix}$, where σ is the interest radius. The initial interest distribution indicates that the data closer to the hurricane's center provides the most relevant data, and the interest for the data from a particular location x decreases according to its radial distance to the center.

3.2.1. Interest function update

The interest function indicates to the controller where it is most beneficial to allocate the balloon for the next time step. To avoid assigning a balloon to a region where another balloon is already collecting data, the interest function must be adjusted according to the locations of the balloons. Dynamically, as a balloon approaches a given position, the value of the interest function at that point is expected to decrease. After the balloon has passed, the value should return to its original state. This time-evolution behavior of the interest function $\Gamma(q(t), x, t)$ is captured by the following update law:

$$\frac{\partial \Gamma(\mathbf{q}(t), \mathbf{x}, t)}{\partial t} = \Psi(\mathbf{q}(t), \mathbf{x}, t)$$

$$- \sum_{i=1}^{2} \frac{\partial}{\partial x_{i}} \left[g_{i}(\mathbf{x}) \Gamma(\mathbf{q}(t), \mathbf{x}, t) \right]$$

$$+ \sum_{i=1}^{2} \sum_{j=1}^{2} \frac{\partial^{2}}{\partial x_{i} \partial x_{j}} \left[D_{ij}(\mathbf{x}) \Gamma(\mathbf{q}(t), \mathbf{x}, t) \right],$$
(8)

where the first component, $\Psi(q(t), x, t)$, updates $\Gamma(q(t), x, t)$ based on the detection of the balloons' positions, and the second and third components focus on restoring the interest function to its initial value, as described by Eq. (7), where the balloons' influence is no longer present. This restoration law is known as the two-dimensional Fokker–Planck equation. In Eq. (8), $g_i(x)$ is the ith component of the drift vector g(x), and $D_{ij}(x)$ is the (i,j)-th component of the diffusion tensor D(x). The drift vector g(x) is given by

$$g_1(\mathbf{x}) = -\frac{D_{11}}{\sigma^4} \|\mathbf{x}\|^3 \cos \phi,$$
 (9a)

$$g_2(\mathbf{x}) = -\frac{D_{22}}{\sigma^4} \|\mathbf{x}\|^3 \sin \phi, \tag{9b}$$

where $\phi=\tan^{-1}(\frac{x_2}{x_1})$. The drift vector tells us the average direction and speed at which the function $\Gamma(q(t),\mathbf{x},t)$ is "moving" at each point \mathbf{x} . In the context of the hurricane application, it describes how this function changes over time, i.e., how fast it returns to its initial condition. Accordingly, the drift vector depends on the diffusion tensor $D(\mathbf{x})$ because it expresses how the interest function diffuses over time in different directions at a specific position \mathbf{x} . Therefore, defining $g_1(\mathbf{x})$ and $g_2(\mathbf{x})$ as shown in Eq. (9) ensures that as $t \to \infty$, $\Gamma(q(t),\mathbf{x},t)$ approaches its steady-state, balloon-free value.

In more detail, the first updating component of the interest function, which is related to the coverage of the balloons, is given by

$$\Psi(q(t), \mathbf{x}, t) = -\sum_{i=1}^{N} \Phi_i(q_i(t), \mathbf{x})$$
(10)

in which, $\Phi_i(q_i(t), x)$ is the *i*th balloon's coverage influence, described by:

$$\boldsymbol{\Phi}_{i}(\boldsymbol{q}_{i}(t), \boldsymbol{x}) = \frac{1}{(2\pi |\boldsymbol{H}_{i}|)^{1/2}} \exp\left[-\frac{1}{2}\left(\left(\boldsymbol{x} - \boldsymbol{q}_{i}(t)\right)^{T} \boldsymbol{H}_{i}^{-1}\left(\boldsymbol{x} - \boldsymbol{q}_{i}(t)\right)\right)\right], \quad (11)$$

where $H_i = \eta_i^2 \begin{bmatrix} 1 & 0 \\ 0 & 1 \end{bmatrix}$, and η_i is the radius of each observation area, i.e., the area within which each balloon can detect and collect data. Note that the *i*th balloon's coverage influence, given by Eq. (10), is greater at the balloon's location $q_i(t)$ and decreases as the position x is farther from $q_i(t)$.

Finally, the solution of Eq. (8) is normalized at each time instant to ensure that the interest function values always remain between 0 and 1.

3.3. Cost function

The design of the cost function is fundamental, as it will guide the controller in achieving the system's goals. Since the objectives are anchored in both area coverage and communication requirements, two components must be created.

The cost energy, $V_{ac}(q(t),t)$, associated with the area coverage requirement can be expressed as

$$V_{ac}(\boldsymbol{q}(t),t) = \beta_{ac} \left(\frac{A_n(\boldsymbol{q}(t),t)}{A_T} \right), \tag{12}$$

where $A_n(q(t),t) = \int_{x \in \mathcal{X}} \Gamma(q(t),x,t) \mathrm{d}x$ is the remaining interest of the area covered by all the agents, and $A_T = \int_{x \in \mathcal{X}} \Gamma(q(t),x,0) \mathrm{d}x$ is the total interest of the area, where $\mathcal{X} \subset \mathbb{R}^2$ is the studied region. The parameter β_{ac} is the weight of the area coverage component in the cost function.

The communication component, denoted by $V_{cc}(q(t),t)$, should reflect the communication requirement, specifically that the base station receives data from the maximum number of balloons. To mathematically express this requirement, we utilize the cumulative communication matrix $\bar{L}(q(t),t)=(\bar{l}_{ij})$, which records all past interactions between the balloons. The communication component is defined as:

$$V_{cc}(\boldsymbol{q}(t),t) = -\beta_{cc} \left(\bar{l}_{11}(\boldsymbol{q}(t),t) + \gamma \sum_{i \in \mathcal{M}} \bar{l}_{ii}(\boldsymbol{q}(t),t) \right), \tag{13}$$

where $\beta_{cc}(t)$ is the time-dependent weight of $V_{cc}(q(t),t)$ in the cost function, reflecting the increasing urgency for the system to remain connected. $\mathcal{M} \subset 1, \ldots, N$ is the set of balloons designated as routers.

Finally, both requirements can be stacked in a single energy vector

$$V(q(t),t) = \left\| \begin{bmatrix} V_{cc}(q(t),t) \\ V_{ac}(q(t),t) \end{bmatrix} \right\|. \tag{14}$$

3.4. Neural-Network-based MPC (NNMPC)

The control protocol chosen to achieve area coverage and communication is the neural-network-based model predictive control (NNMPC) designed by Floriano et al. (2022). This method has the advantage of operating in random processes and handling unknown external disturbances due to its online learning feature. Additionally, it is designed to work effectively in applications with limited communication capacities.

Due to the presence of stochastic fluctuations, Eq. (14) is stochastic. By taking its expected value and assuming a time horizon H, the MPC cost is

$$J(t) = \int_{\tau=0}^{H} E[V(q(t+\tau), t+\tau)] d\tau.$$
 (15)

For easier computation, we propose solving the discrete-time version of the problem using the neural network approach. Specifically, at each sample time t_k , and assuming a horizon h, we select $u(t_k) \in \mathbb{Z}^N$ from the sequence $u(t_k), \ldots, u(t_{k+h}) \in \mathbb{Z}^{Nh}$ that minimizes the cost function

$$J(t_k) = \sum_{\ell=0}^{h} E\left[V(q(t_{k+\ell}), t_{k+\ell})\right],$$
(16)

while satisfying the discrete-time implementation of dynamical Eqs. (4a)–(4d).

4. Simulation experiments

The codes and results used in this study are available online.²

All simulations were conducted over a time span of $t_{max} = 48$ h, using 501 time samples and 61 spatial steps per dimension within a grid covering a range of 200 km.

The communication range of the balloons was set to $\rho=10$ km, consistent with the capabilities of LoRa as detailed in Section 3.1.

In terms of area coverage, we set $\sigma = 100$ km and $\eta_i = 10$ km for all $i \in 1, ..., N$. In the Fokker–Planck equation, $D_{11} = D_{22} = 1$.

The hurricane parameters used in Eq. (4d) were set as $\phi = 1.8$, $\chi = 0.5$, $V_m = 60$ m/s, and $R_V = 20$ km, based on a baseline profile described by Holland et al. (2010).

The control parameters were set with a level height $\bar{z}=558.3$ m, consistent with the three-level control described by Meneghello et al. (2016, 2018). Additionally, $\alpha=10^{-3}$ s⁻¹, $c^2=1500$ m²/s, $\beta_{ac}=1$, and $\beta_{cc}=1$ were used. Finally, a predictive horizon of h=10 was selected for the control strategy.

Regarding the neural network architecture employed in the control framework, several strategic choices were made to balance performance and efficiency. A feed-forward neural network with a single hidden layer was utilized. This structure provides a suitable balance between model complexity and computational demands, ensuring the network can capture essential patterns without overfitting or introducing unnecessary delays in real-time processing.

The network consisted of M=6 neurons in the hidden layer, a configuration that provides sufficient representational capacity to model the system's underlying dynamics while keeping the model lightweight and responsive. The hyperbolic tangent (tanh) activation function was selected for its smooth, non-linear properties, which are particularly effective for handling varied input data and enhancing the network's ability to generalize well across different scenarios.

Finally, the stopping criterion for the training process was set to J in Eq. (16) being less than or equal to 10. This ensured that the model met the required performance standards without excessive training time. This criterion was established to maintain a high level of accuracy while also allowing the network to adapt quickly to the dynamic conditions presented by the control problem.

4.1. Simulation with N = 9

In this subsection, a total of N=9 balloons were employed (including the base station). The simulation was conducted with $T_{cc}=T=6$ h. Fig. 3 displays 6 instances of the simulation, each separated by 100 time steps. Each subfigure presents a heatmap of the interest function at that specific time, with each point representing one of the ith balloons. Observe the contrasting patterns in the figures: some depict the balloons in clusters, while others show them dispersed across the hurricane's area. This variation directly reflects the coverage/communication trade-off. The balloons periodically and interchangeably gather to establish communication links and then disperse to extend the covered area. This dynamic adaptation allows the

² Available at https://github.com/brunofloriano/NN_MPC_application.

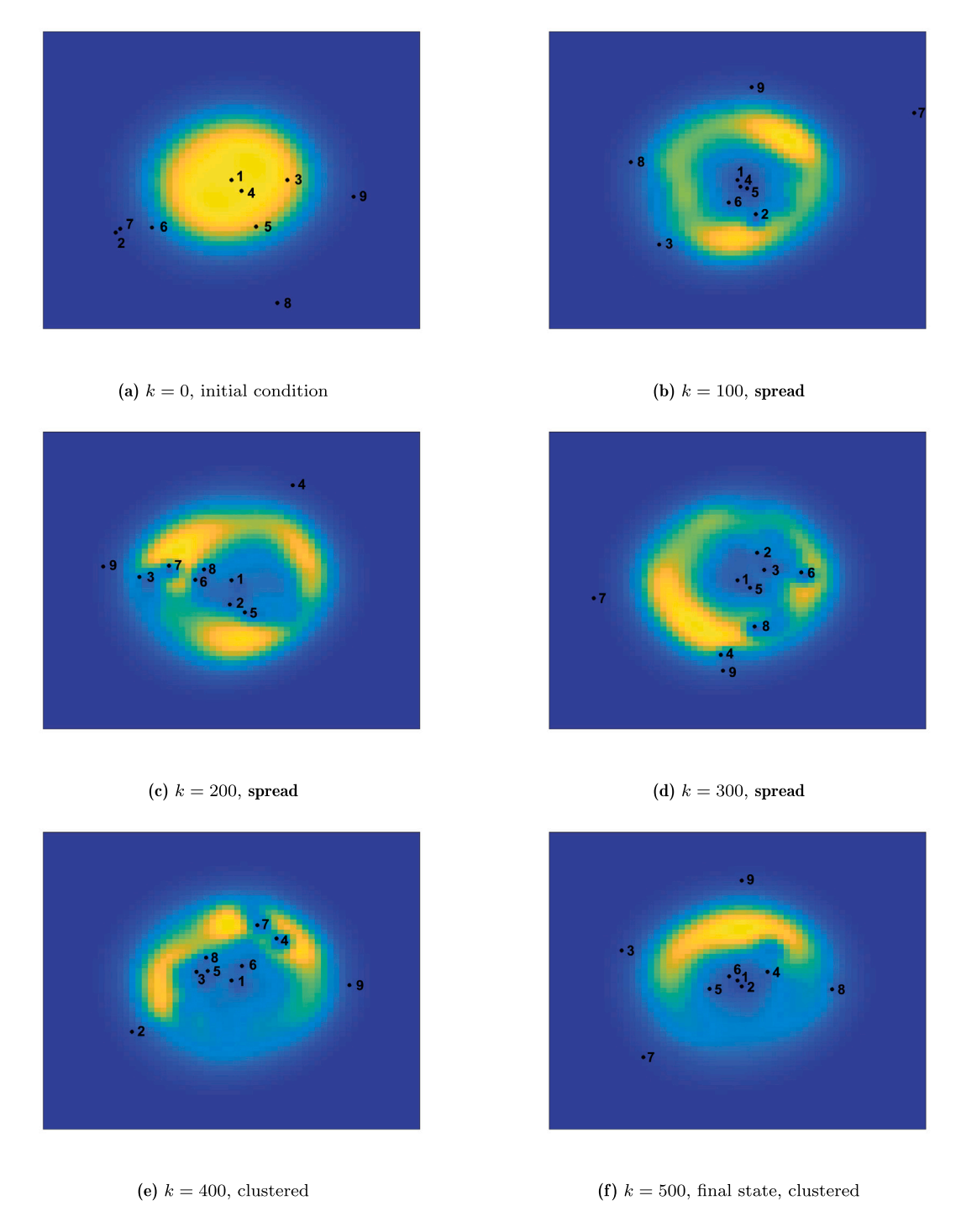


Fig. 3. Interest function at different time steps. Compare the differences when the balloons are: clustered (indicating the communication priority) or spread (area coverage priority).

system to address each objective according to the specific needs at each moment.

In addition to Fig. 3, Table 1 provides complementary information. For each time step shown in the figure, a communication relative size is given by a numerical value. This parameter, referred to as the communication relative energy, represents the proportion of the communication energy $V_{cc}(q(t),t)$ relative to the total energy vector V(q(t),t). It is calculated as follows

$$E_{cc}(q(t),t) = \frac{V_{cc}(q(t),t)}{V(q(t),t)}.$$
(17)

Table 1 Communication relative size, $E_{cc}(q(t_k), t_k)$, at each time step k. The maximum value occurs when the balloons are spread.

Time step k	$E_{cc}(\boldsymbol{q}(t_k),t_k)$	Situation
0	-0.0330	Initial condition
100	-0.1991	Spread
200	-0.2126	Spread
300	-0.1481	Spread
400	-0.3053	Clustered
500	-0.4051	Clustered

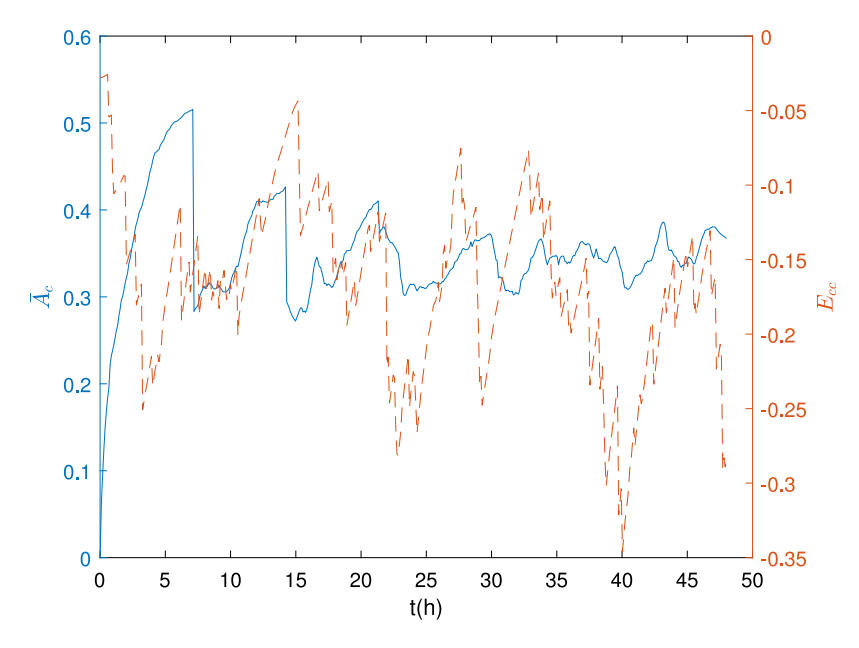


Fig. 4. Cumulative area covered by the system, \bar{A}_c (solid line), and communication energy, V_{cc} (dashed line), over time with $T_{cc} = 6$ h. Notice the periodicity in both curves, indicating the compromise between area coverage and communication.

A smaller value indicates that the balloons are positioned closer together, prioritizing the establishment of communication links. Conversely, higher values correspond to situations where the balloons are spread out, emphasizing area coverage. In this paper, we define a threshold of $E_{cc}(q(t),t)=-0.25$ to categorize the scenarios: values above this threshold indicate that the system is in a scattering situation (agents are spread out), while values below it signify a clustered situation (agents are closer together). An exception occurs at k=0 (the initial condition), where the system is in its early stage, and both coverage and communication may have similar priorities due to their low achievement levels at this point.

In order to perform a correct analysis of the area coverage cycles, let the cumulative interest be given by

$$\bar{A}_n(q(t),t) = \min_{\tau} A_n(q(\tau),\tau),\tag{18}$$

where $\tau \in \begin{bmatrix} t - T_{ac} & t \end{bmatrix}$ and T_{ac} is the area coverage period. Then, the cumulative area covered can be defined as

$$\bar{A}_{c}(q(t),t) = 1 - \frac{\bar{A}_{n}(q(t),t)}{A_{T}}.$$
 (19)

Therefore, our analysis will focus on cycles of the same duration, i.e., $T_{ac} = T_{cc}$. Fig. 4 shows the cumulative area covered, $\bar{A}c$, and the communication relative energy, E_{cc} , with $T_{ac} = T_{cc} = 6$ h, by the system over time.

Notice the oscillating tendency of both curves. This oscillation is due to the restoring cost function, influenced by the linear decay in the communication component of Eq. (13), and the dynamics of the interest function governed by the Fokker–Planck equation described in Section 3.2.1. This combination causes the interest function to gradually return to its initial state.

As expected, both curves follow a similar pattern. As the balloons cover the interest area, $\bar{A}_c(q(t),t)$ increases. However, this increase also elevates the communication energy, because past connections become significantly degraded. The communication energy decreases when the agents reposition to establish connections, but this comes at the cost of losing previously covered areas.

As an illustration, refer to Fig. 5. It depicts the exact moment when the communication energy is at its minimum (step 418). At this point, you can observe how the balloons are clustered: agents 1, 4, 5, 6, and 8 form one cluster, while 3, 7, and 9 form another, with agent 2 being isolated. This configuration highlights the system's focus on enhancing

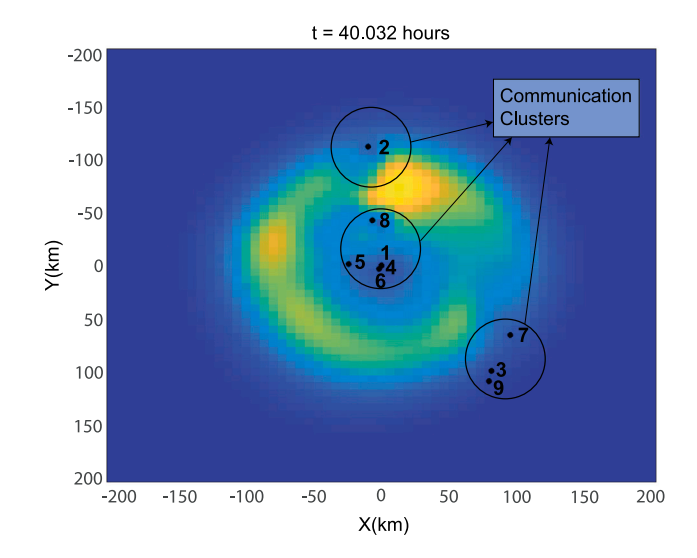


Fig. 5. Interest function when communication energy is at a minimum. Notice how the balloons are gathered in clusters, indicating they are prioritizing communication.

communication at the expense of area coverage. Following this step, the system reorganizes, and the balloons disperse to resume area coverage.

Fig. 6 shows the cumulative area covered, $\bar{A}c$, and the communication relative energy, E_{cc} , with $T_{ac}=T_{cc}=12\mathrm{h}$ over time. The extended time period enhances the visualization of the synchronization between the two objectives.

4.2. Simulation with N=4

For the next portion, we will reduce the number of agents to more clearly illustrate the message routing process. This adjustment will allow us to better visualize how the agents redirect messages when necessary. With fewer agents, the demonstration becomes more straightforward and illustrative. We will use the same parameters as before, except with N=4 and $T_{cc}=6$ h. Here, we introduce the concept of a "connection frame", which is the time window during which a connection retains more than 60% of its strength. Specifically,

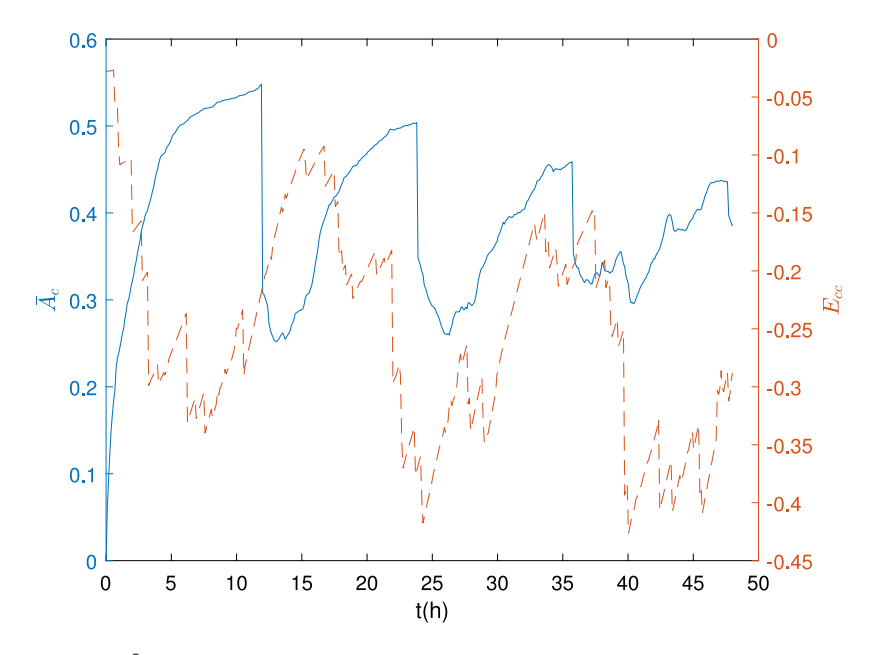


Fig. 6. Cumulative area covered by the system, \bar{A}_c (solid line), and communication energy, V_{cc} (dashed line), over time with $T_{cc}=12$ h. Notice the synchronization between the two objectives.

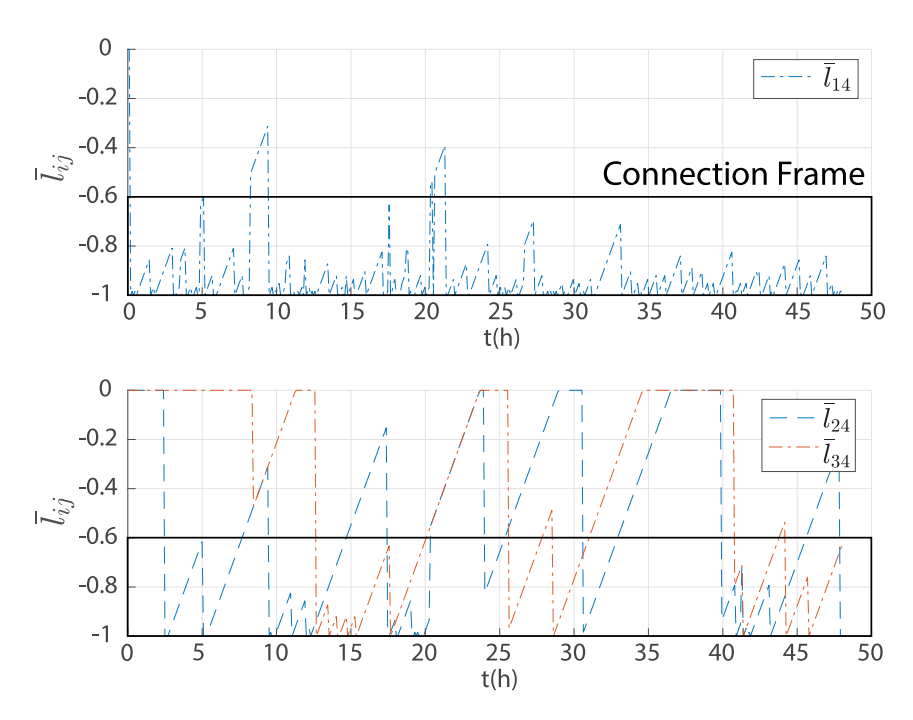


Fig. 7. Entries \bar{l}_{ij} of the cumulative Laplacian matrix $\bar{L}(q(t),t)$. Notice how the router j=4 is mostly connected to the base station (i=1) and have intermittent connections with other agents.

 \bar{l}_{ij} remains between -0.6 and -1. This interval indicates the steadiness of the connection between agents i and j, providing insight into the consistency of their communication link.

Fig. 7 shows the entries \bar{l}_{ij} of the cumulative Laplacian matrix $\bar{L}(q(t),t)$. In this example, agent j=4 acts as the routing agent, which is why its connection to the base station (represented by \bar{l}_{14}) remains almost constant, as seen in the top graph. During most of the simulation, \bar{l}_{14} stays within the connection frame. Additionally, the bottom graph shows that agents 2 and 3, which are coverage-only balloons, have intermittent connections with agent 4 to periodically send their data. This setup ensures that the data ultimately reaches the base station, demonstrating how messages are forwarded between the balloons to guarantee that all observations are sent to the base station.

4.3. Discussion

The results from the proposed Neural Network Model Predictive Control (NNMPC) system provide several key insights into its effectiveness for hurricane monitoring. Observations from the simulations reveal distinct patterns in the balloons' positions, with some configurations forming clusters and others being more dispersed. This variation underscores the system's ability to dynamically balance the trade-off between communication and area coverage. The balloons periodically regroup to establish strong communication links and then spread out to maximize area coverage, effectively addressing each objective based on current needs.

The oscillatory nature of the coverage and communication curves can be attributed to the dynamics of the cost function. This cost function is influenced by the linear decay in the communication component and the Fokker–Planck equation that governs the area of interest, leading to periodic adjustments. This behavior reflects the system's efforts to balance the competing goals of communication efficiency and coverage optimization. The Fokker–Planck equation models the recency of information, allowing the interest function to revert to its initial state and contributing to the observed oscillations.

A complementary relationship between coverage and communication energy is evident from the results. As the balloons cover a larger portion of the target area, the coverage metric increases, which typically leads to a rise in communication energy due to the degradation of previously established connections. The system mitigates this by reducing communication energy when the balloons reposition to reestablish connections, although this results in a temporary reduction in covered areas. This balance highlights the system's efficiency in managing the trade-off between data acquisition and communication.

Overall, the results confirm the effectiveness of the NNMPC approach in balancing the complex trade-off between coverage and communication. The system's ability to adapt in real-time and make proactive adjustments based on current and predicted conditions is crucial for successful operation in the challenging environment of hurricane monitoring.

5. Conclusion

This paper introduces a multi-agent control architecture for a swarm of heterogeneous, low-cost buoyancy-driven balloons designed to monitor and collect weather data on hurricanes. The proposed method features two continuously restoring cost function components: one representing communication energy and the other representing area coverage energy. The control scheme utilizes neural-network-based model predictive control (MPC) and three-level control (TLC) to create an adaptive multi-agent framework that optimizes the cost function.

The proposed method was tested in a simulated environment over two distinct periods, each lasting 48 h. In both cases, clear cycles and expected synchronization between area coverage and communication were observed. The trade-off between these conflicting objectives was effectively managed, as the multi-agent system (MAS) adaptively switched between them to better address the problem.

Future research directions include validating the proposed protocol on real platforms to evaluate its performance with actual vehicles. Additional investigations could focus on adapting the system to various initial conditions, examining how balloons are deployed within the hurricane and retrieved after measurements are completed. Moreover, enhancing the current system might involve integrating a robust adaptation component into the neural network learning process to improve scalability and adaptability, optimizing communication protocols, and refining algorithmic parameters. Finally, exploring the use of deep learning and other artificial intelligence techniques is recommended to expand the range of solutions for the current problem. These research efforts collectively aim to enhance the reliability, adaptability, and practical applicability of the proposed protocol.

CRediT authorship contribution statement

Bruno R.O. Floriano: Conceptualization, Data curation, Formal analysis, Investigation, Methodology, Software, Validation, Visualization, Writing – original draft, Writing – review & editing, Funding acquisition. **Benjamin Hanson:** Methodology, Software, Visualization, Writing – original draft. **Thomas Bewley:** Conceptualization, Methodology, Project administration, Resources, Supervision, Writing – original draft. **João Y. Ishihara:** Conceptualization, Formal analysis, Funding acquisition, Investigation, Methodology, Project administration, Resources, Supervision, Validation, Writing – original draft, Writing

– review & editing. **Henrique C. Ferreira:** Conceptualization, Formal analysis, Funding acquisition, Investigation, Methodology, Project administration, Resources, Supervision, Validation, Writing – original draft, Writing – review & editing.

Declaration of competing interest

The authors declare the following financial interests/personal relationships which may be considered as potential competing interests: Bruno Rodolfo de Oliveira Floriano reports financial support was provided by Coordenação de Aperfeiçoamento de Pessoal de Nível Superior. Joao Yoshiyuki Ishihara reports financial support was provided by Conselho Nacional de Desenvolvimento Científico e Tecnológico.

Acknowledgments

This work was supported in part by Conselho Nacional de Desenvolvimento Científico e Tecnológico CNPq, Brazil, under grant 316487/2021-0/PQ and Coordenação de Aperfeiçoamento de Pessoal de Nível Superior, CAPES, Brazil, under grants 8881.690053/2022-01 and 88887.510939/2020-00.

Data availability

The associated data/code is available in a link included in the paper.

References

- Afghah, F., Razi, A., Chakareski, J., Ashdown, J., 2019. Wildfire monitoring in remote areas using autonomous unmanned aerial vehicles. In: IEEE INFOCOM 2019 IEEE Conference on Computer Communications Workshops (INFOCOM WKSHPS). IEEE, Paris, France, pp. 835–840. http://dx.doi.org/10.1109/INFCOMW.2019.8845309.
- Baldazo, D., Parras, J., Zazo, S., 2019. Decentralized multi-agent deep reinforcement learning in swarms of drones for flood monitoring. In: 2019 27th European Signal Processing Conference (EUSIPCO). IEEE, A Coruna, Spain, pp. 1–5. http://dx.doi. org/10.23919/EUSIPCO.2019.8903067.
- Bewley, T., Meneghello, G., 2016. Efficient coordination of swarms of sensor-laden balloons for persistent, in situ, real-time measurement of hurricane development. Phys. Rev. Fluids 1 (6), 060507.
- Cione, J.J., Kalina, E., Uhlhorn, E., Farber, A., Damiano, B., 2016. Coyote unmanned aircraft system observations in Hurricane Edouard (2014). Earth Space Sci. 3 (9), 370–380.
- Congress, S., Puppala, A.J., Banerjee, A., Jafari, N.H., Patil, U.D., 2019. Use of unmanned aerial photogrammetry for monitoring low-volume roads after Hurricane Harvey. In: 12th International Conference on Low-Volume Roads. Vol. 530.
- Das, A., Gervet, T., Romoff, J., Batra, D., Parikh, D., Rabbat, M., Pineau, J., 2019. Tarmac: Targeted multi-agent communication. In: International Conference on Machine Learning. PMLR, pp. 1538–1546.
- Day, R., Salmon, J., 2021. A framework for multi-UAV persistent search and retrieval with stochastic target appearance in a continuous space. J. Intell. Robot. Syst. 103 (4), 65.
- Eshaghi, K., Nejat, G., Benhabib, B., 2023. A concurrent mission-planning methodology for robotic swarms using collaborative motion-control strategies. J. Intell. Robot. Syst. 108 (2), 15.
- Floriano, B.R.O., Borges, G.A., Ferreira, H.C., Ishihara, J.Y., 2021. Hybrid Dec-POMDP/PID guidance system for formation flight of multiple UAVs. J. Intell. Robot. Syst. 101 (3), 1–20.
- Floriano, B.R., Vargas, A.N., Ishihara, J.Y., Ferreira, H.C., 2022. Neural-network-based model predictive control for consensus of nonlinear systems. Eng. Appl. Artif. Intell. 116, 105327.
- Fuertes, D., del-Blanco, C.R., Jaureguizar, F., Navarro, J.J., García, N., 2023. Solving routing problems for multiple cooperative Unmanned Aerial Vehicles using Transformer networks. Eng. Appl. Artif. Intell. 122, 106085. http://dx.doi.org/10.1016/ i.engappai.2023.106085.
- Ghazali, M.H.M., Teoh, K., Rahiman, W., 2021. A systematic review of real-time deployments of UAV-based LoRa communication network. IEEE Access 9, 124817–124830. http://dx.doi.org/10.1109/ACCESS.2021.3110872.
- Gong, B., Jiang, T., 2011. A tree-based routing protocol in wireless sensor networks. In: 2011 International Conference on Electrical and Control Engineering. IEEE, pp. 5729–5732.
- Greenwood, F., Nelson, E.L., Greenough, P.G., 2020. Flying into the hurricane: A case study of UAV use in damage assessment during the 2017 hurricanes in Texas and Florida. PLoS one 15 (2), e0227808.

- Holland, G.J., Belanger, J.I., Fritz, A., 2010. A revised model for radial profiles of hurricane winds. Mon. Weather Rev. 138 (12), 4393–4401.
- Hu, W., Liu, L., Feng, G., 2018. Cooperative output regulation of linear multi-agent systems by intermittent communication: A unified framework of time- and eventtriggering strategies. IEEE Trans. Autom. Control 63 (2), 548–555. http://dx.doi. org/10.1109/TAC.2017.2727821.
- Hu, J., Niu, H., Carrasco, J., Lennox, B., Arvin, F., 2022. Fault-tolerant cooperative navigation of networked UAV swarms for forest fire monitoring. Aerosp. Sci. Technol. 123, 107494. http://dx.doi.org/10.1016/j.ast.2022.107494.
- Lin, Z., Liu, H.H., 2018. Topology-based distributed optimization for multi-UAV cooperative wildfire monitoring: Topology-based distributed optimization for multi-UAV cooperative wildfire monitoring. Optim. Control Appl. Methods 39 (4), 1530–1548. http://dx.doi.org/10.1002/oca.2424.
- Manoharan, A., Sujit, P., 2022. Nonlinear model predictive control framework for cooperative three-agent target defense game. arXiv preprint arXiv:2207.09136.
- Meneghello, G., Bewley, T., de Jong, M., Briggs, C., 2017. A coordinated balloon observation system for sustained in-situ measurements of hurricanes. In: 2017 IEEE Aerospace Conference. IEEE, pp. 1–6.
- Meneghello, G., Luchini, P., Bewley, T., 2016. On the control of buoyancy-driven devices in stratified, uncertain flowfields. In: International Symposium on Stratified Flows. Vol. 1.
- Meneghello, G., Luchini, P., Bewley, T., 2018. A probabilistic framework for the control of systems with discrete states and stochastic excitation. Automatica 88, 113–116.
- Mohsan, S.A.H., Othman, N.Q.H., Li, Y., Alsharif, M.H., Khan, M.A., 2023. Unmanned aerial vehicles (UAVs): practical aspects, applications, open challenges, security issues, and future trends. Intell. Serv. Robot. 1–29.
- Petajajarvi, J., Mikhaylov, K., Roivainen, A., Hanninen, T., Pettissalo, M., 2015. On the coverage of LPWANs: range evaluation and channel attenuation model for LoRa technology. In: 2015 14th International Conference on Its Telecommunications. ITST, IEEE, pp. 55–59.
- Puente-Castro, A., Rivero, D., Pazos, A., Fernandez-Blanco, E., 2022. A review of artificial intelligence applied to path planning in UAV swarms. Neural Comput. Appl. 34 (1), 153–170. http://dx.doi.org/10.1007/s00521-021-06569-4.
- Queralta, J.P., Taipalmaa, J., Pullinen, B.C., Sarker, V.K., Gia, T.N., Tenhunen, H., Gabbouj, M., Raitoharju, J., Westerlund, T., 2020. Collaborative multi-robot search and rescue: Planning, coordination, perception, and active vision. IEEE Access 8, 191617–191643.
- Ramirez-Atencia, C., Camacho, D., 2019. Constrained multi-objective optimization for multi-UAV planning. J. Ambient Intell. Humaniz. Comput. 10 (6), 2467–2484. http://dx.doi.org/10.1007/s12652-018-0930-0.
- Rojas, S.S., Khan, S.D., Shahtakhtinskiy, A., 2022. Impact of hurricane harvey on the upper Texas Coast: Using airborne lidar data sets with UAV-derived topographic data to monitor change and track recovery. Remote Sens. 14 (21), 5357.
- Sabir, Z., Babatin, M.M., Hashem, A.F., Abdelkawy, M.A., Salahshour, S., Umar, M., 2024a. Design of stochastic neural networks for the fifth order system of singular engineering model. Eng. Appl. Artif. Intell. 133, 108141.
- Sabir, Z., Khan, S.N., Raja, M.A.Z., Babatin, M.M., Hashem, A.F., Abdelkawy, M.A., 2024b. A reliable neural network framework for the Zika system based reservoirs and human movement. Knowl.-Based Syst. 292, 111621.
- Sabir, Z., Rada, T.B., Kassem, Z., Umar, M., Salahshour, S., 2024c. A novel radial basis neural network for the Zika virus spreading model. Comput. Biol. Chem. 108162.
- Sabir, Z., Umar, M., Wahab, H.A., Bhat, S.A., Unlu, C., 2024d. Heuristic computing performances based Gudermannian neural network to solve the eye surgery corneal model. Appl. Soft Comput. 157, 111540.

- Sanchez-Iborra, R., Cano, M.-D., 2016. State of the art in LP-WAN solutions for industrial IoT services. Sensors 16 (5), 708.
- Saraereh, O.A., Alsaraira, A., Khan, I., Uthansakul, P., 2020. Performance evaluation of UAV-enabled LoRa networks for disaster management applications. Sensors 20 (8), 2396. http://dx.doi.org/10.3390/s20082396.
- Schaefer, M., Teeuw, R., Day, S., Zekkos, D., Weber, P., Meredith, T., Van Westen, C.J., 2020. Low-cost UAV surveys of hurricane damage in dominica: automated processing with co-registration of pre-hurricane imagery for change analysis. Natl. Hazards 101 (3), 755–784.
- Seraj, E., Silva, A., Gombolay, M., 2022. Multi-UAV planning for cooperative wild-fire coverage and tracking with quality-of-service guarantees. Auton. Agents Multi-Agent Syst. 36 (2), 39. http://dx.doi.org/10.1007/s10458-022-09566-6.
- Shi, Y., Hu, J., Wu, Y., Ghosh, B.K., 2023. Intermittent output tracking control of heterogeneous multi-agent systems over wide-area clustered communication networks. Nonlinear Anal. Hybrid Syst. 50, 101387. http://dx.doi.org/10.1016/j. nahs.2023.101387.
- Stampa, M., Sutorma, A., Jahn, U., Thiem, J., Wolff, C., Röhrig, C., 2021. Maturity levels of public safety applications using unmanned aerial systems: a review. J. Intell. Robot. Syst. 103, 1–15.
- Tang, J., Duan, H., Lao, S., 2023. Swarm intelligence algorithms for multiple unmanned aerial vehicles collaboration: A comprehensive review. Artif. Intell. Rev. 56 (5), 4295–4327. http://dx.doi.org/10.1007/s10462-022-10281-7.
- Tzoumas, G., Pitonakova, L., Salinas, L., Scales, C., Richardson, T., Hauert, S., 2023. Wildfire detection in large-scale environments using force-based control for swarms of UAVs. Swarm Intell. 17 (1–2), 89–115. http://dx.doi.org/10.1007/s11721-022-00218-9.
- Viseras, A., Meissner, M., Marchal, J., 2021. Wildfire front monitoring with multiple UAVs using deep Q-learning. IEEE Access 1. http://dx.doi.org/10.1109/ACCESS. 2021.3055651.
- Vizcaya-Martínez, D.A., Flores-de Santiago, F., Valderrama-Landeros, L., Serrano, D., Rodríguez-Sobreyra, R., Álvarez-Sánchez, L.F., Flores-Verdugo, F., 2022. Monitoring detailed mangrove hurricane damage and early recovery using multisource remote sensing data. J. Environ. Manag. 320, 115830.
- Wang, L., Wang, K., Pan, C., Xu, W., Aslam, N., Hanzo, L., 2020. Multi-agent deep reinforcement learning-based trajectory planning for multi-UAV assisted mobile edge computing. IEEE Trans. Cogn. Commun. Netw. 7 (1), 73–84.
- Wen, G., Duan, Z., Ren, W., Chen, G., 2014. Distributed consensus of multi-agent systems with general linear node dynamics and intermittent communications. Internat. J. Robust Nonlinear Control 24 (16), 2438–2457. http://dx.doi.org/10. 1002/rnc.3001.
- Wu, Y., Xu, S., Dai, W., Lin, L., 2023. Heuristic position allocation methods for forming multiple UAV formations. Eng. Appl. Artif. Intell. 118, 105654. http: //dx.doi.org/10.1016/j.engappai.2022.105654.
- Xiao, S., Dong, J., 2021. Distributed fault-tolerant tracking control for heterogeneous nonlinear multi-agent systems under sampled intermittent communications. J. Franklin Inst. 358 (17), 9221–9242. http://dx.doi.org/10.1016/j.jfranklin.2021.08. 019.
- Yeom, J., Han, Y., Chang, A., Jung, J., 2019. Hurricane building damage assessment using post-disaster UAV data. In: IGARSS 2019-2019 IEEE International Geoscience and Remote Sensing Symposium. IEEE, pp. 9867–9870.
- Zhang, P., Xue, H., Gao, S., Zhang, J., 2021. Distributed adaptive consensus tracking control for multi-agent system with communication constraints. IEEE Trans. Parallel Distrib. Syst. 32 (6), 1293–1306. http://dx.doi.org/10.1109/TPDS.2020.3048383.